AXON VOLTAGE-CLAMP SIMULATIONS

IV. A MULTICELLULAR PREPARATION

FIDEL RAMÓN, NELS ANDERSON, RONALD W. JOYNER, *and* JOHN W. MOORE

From the Department of Physiology and Pharmacology, Duke University Medical Center, Durham, North Carolina 27710

ABSTRACT In this paper we extend the simulation of the voltage clamp of a single nerve fiber to a bundle of axons. These simulations included not only the description of the voltage clamp circuit and a single unidimensional cable to represent the preparation in the "node" region of a double sucrose gap used previously but also a series resistance and a shunt pathway. The output of the voltage control amplifier is applied across the membrane plus the series resistance, producing a voltage drop across the series resistance due to the current generated by the membrane in response to a depolarizing voltage step. Since the membrane current has an inward and an outward phase, voltage drops of opposite sign are produced across the series resistance. During the transient current and at all points along an axon, the potential deviation produced by the series resistance is opposite to the deviation produced by the longitudinal gradient. Only at a command potential equal to the sodium equilibrium potential, the membrane potential transiently matches the command potential. For the attempted voltage clamp of an axon, values of series resistance larger than 50 Ω-cm^2 allowed propagated action potentials in the membrane. In spite of the presence of propagated action potentials at the cable membrane, the recorded current does not show "notches" and it has a phase of inward current and a phase of outward current. It is concluded that, in a multicellular preparation with series resistance, the recording of a square voltage pulse does not indicate voltage control of the transmembrane potential. The presence of a shunt pathway produces inaccurate values of current density. Neither series or shunt resistance produce "notches" in the current records.

INTRODUCTION

In the second of this sequence of papers, we presented the results of a simulated voltage clamp of a single unidimensional cable. This cable, for the configuration where current and voltage recording electrodes were placed at the ends of the cable, was taken as the model of a nerve in the double sucrose-gap voltage clamp. (Moore et al., 1975 *b*).

The purpose of this paper is to describe the simulations of a multicellular preparation of parallel fibers such as the lobster leg nerve, in a double sucrose-gap voltage clamp similar to that described for a single nerve. It includes the additional complications of a series resistance as well as the necessary shunt resistance. Such a preparation is of interest not only for its own sake but also because it can be taken as a biological model of a syncytial tissue (smooth muscle).

The double sucrose-gap technique has also been applied to multicellular preparations with intercellular electrical connections such as smooth muscle (Anderson, 1969) and cardiac muscle (Rougier et al., 1968), that behave in some respects as a single fiber due to their syncytial properties. For simplicity, unidimensional cable theory has been used for the analysis of syncytial preparations (Tomita, 1966; Abe and Tomita, 1968). However, it has not been clearly established that a unidimensional cable is a model of a syncytial preparation (Tarr and Trank, 1974). In order to have a better understanding of the behavior of a syncytial preparation in the double sucrose gap, we took an intermediate step, the simulation of the voltage clamp of a preparation (unmyelinated nerve) which we know can be approximated by unidimensional cables in parallel.

The rationale for using a nerve trunk as a simplified model of a syncytial preparation (smooth muscle) in the double sucrose gap, is as follows: if one assumes that in a strip of smooth muscle all the cells are arranged in parallel fashion and that their membranes have the same electrical characteristics, then the strip of muscle can be considered as composed of a number of uniform interconnected parallel cells. In such an array, the simultaneous injection of current into all the cells would produce similar voltage gradients in each cell, so that the transversal couplings can be disregarded. Longitudinal couplings can also be disregarded, since the minimum practical "node" length of the sucrose gap is approximately the length of a single smooth muscle cell (about 150 μm) and the junctional area is not large enough (about 0.05% of the total surface area) as to decrease significantly the cell surface area.[1] For simplicity a single unidimensional cable, such as that reported in the second of the present series of papers, might seem sufficient.

However, in order to have a better representation of the experimental conditions, at least two more components have to be added to the circuit. These extra components are: a resistance in series with the membrane (R_s) and a shunt resistance (R_{Sh}) between the current injecting and the recording electrodes.

The presence of a resistance in series with the membrane introduces complications to many studies conducted with the voltage clamp. Typically, the curve of h_∞ as usually measured (Hodgkin and Huxley, 1952) appears to be shifted in the hyperpolarizing direction along the voltage axis. This result was analyzed by one of us (J. W. Moore) and has been previously referred to (Goldman and Schauf, 1972). However, since most of these effects are the result of the lack of voltage control across the membrane, in this paper we will limit ourselves to describe the effects of a resistance in series with the membrane on the membrane voltage and net currents. Some of the causes of voltage inhomogeneity under voltage clamp conditions have also been analyzed for cardiac muscle preparations (Johnson and Lieberman, 1971).

METHODS

The equations that describe the system, and the numerical methods used for the solution of the partial and ordinary differential equations, are basically the same as described previously

[1] Zampighi, G., F. Ramón, and N. Anderson. 1974. In preparation.

(Moore et al., 1975 *a*). However, here we use the standard H-H values for $\bar{g}_{Na}$ and $\bar{g}_K$, except for Figs. 1 and 2. We will also define depolarizing deviations of the transmembrane voltage as positive deviations and hyperpolarizing deviations as negative deviations.

RESULTS

Series Resistance

When a resistance is added in series with the membrane, the equivalent circuit of the preparation is shown in Fig. 1 A. Voltage command pulses are now applied across the whole circuit and not just across the membrane.

Hodgkin et al. (1952) observed a resistance of 7 Ω-cm^2 in series with the active membrane of the squid axon. This is usually attributed to the Schwann cell layer which is closely wrapped around the axon. The series resistance has a negligible effect on the shape of the action potential in a current clamp but it introduces a marked effect on the shape and magnitude of currents in a voltage clamp. Hodgkin et al. (1952) were able to measure and, on the average, compensate for 70% of this resistance and thus arrive at currents which reflected the true membrane characteristics much more accurately. The effects of such compensation are shown for one potential in their Fig. 17. The Hodgkin and Huxley (H-H, 1952) equations then actually represent the characteristics of a membrane with a series resistance of only 2 Ω-cm^2 and therefore are usually taken as representing the membrane itself.

In the following pages we will discuss the effects of a resistance in series with the membrane, on the current and voltage records obtained during voltage clamp conditions. For these examples we will take the H-H model, without modifications, as the representation of the membrane. It is obvious that if the conductances are increased by a factor of 2 as we did in the second paper of this series (Moore et al., 1975 *b*) to simulate the squid giant axon membrane, the deviations of the voltage records from the command potential, and therefore those of the current records, would be much greater.

Single Membrane Patch. The current produced by the membrane in response for depolarizing command voltages less than the sodium equilibrium potential has two phases, a transient phase of inward current and a steady-state of outward current. During those two phases, the current flows in opposite directions across the series resistance and voltage changes of opposite sign are produced across the series resistance (Fig. 1 B).

Across the series resistance the voltage drop is negative during the transient phase of inward current, and it becomes positive during the phase of outward current. At voltage commands greater than the sodium equilibrium potential the current through the membrane is always outward, and the voltage drop across the series resistance is always positive. At a command potential equal to the sodium equilibrium potential, there is no current flowing across the series resistance during the transient phase and no voltage drop is produced then. Therefore the sodium equilibrium potential is the only potential at which the voltage across the membrane transiently matches the command pulse. The transmembrane voltages resulting from these effects are shown in Fig. 1 C.

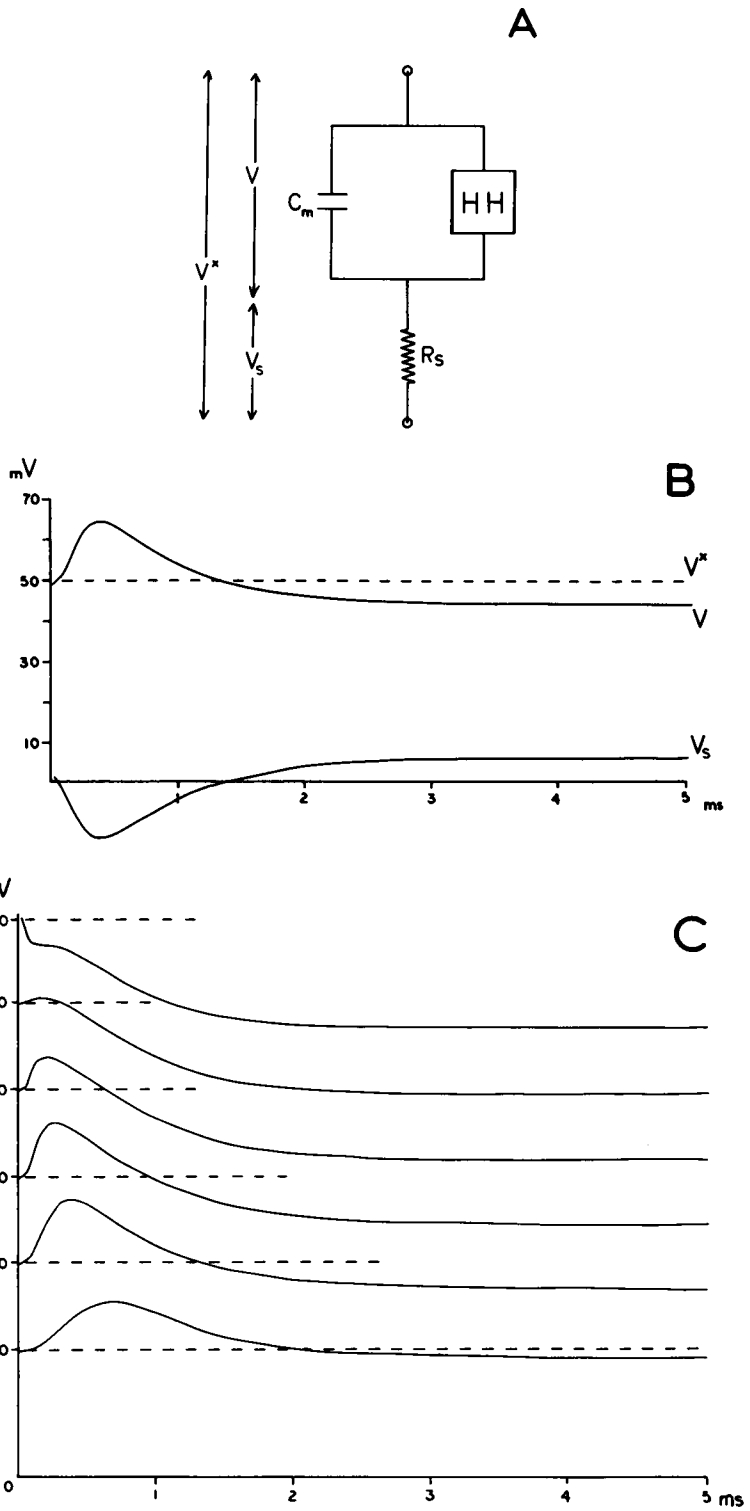
A
V*
V
Vs
Cm
HH
Rs
B
mV
70
50
30
10
V*
V
Vs
1
2
3
4
5
ms
C
mV
130
110
90
70
50
30
0
1
2
3
4
5 ms

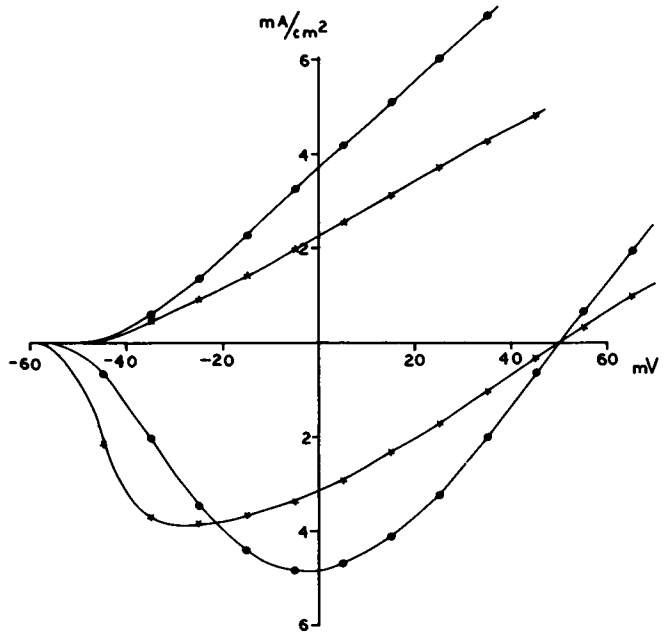

FIGURE 2 Transient and steady-state current-voltage relationship for a membrane patch. The control, with a $R_s = \phi$ Ω-cm^2 (circles) is compared with the same membrane patch with a $R_s = 7$ Ω-cm^2 (stars). Note the shift of the transient current curve to the left along the voltage axis. The reversal potential of the transient current remains unchanged. To emphasize the effect of the series resistance, this computation was performed increasing the sodium and potassium conductances by a factor of 2 and the holding potential 20 mV hyperpolarized.

The transient current-voltage (I-V) relationship resulting from a simulated voltage clamp of the equivalent circuit of the membrane plus series resistances of ϕ and 7 Ω-cm^2 can be seen in Fig. 2. Because of the deviations of the transmembrane voltage from the command pulse, the I-V relationship appears shifted to the left on the voltage axis. The amount of shift is proportional to the value of the series resistance. Since the whole curve swings around the sodium equilibrium potential, there is a range of potentials at which the resulting current is larger than when the series resistance is zero (control) and another at which it is smaller than the control. In the region in which the resulting current is larger than the control, the series resistance effect can be so large

FIGURE 1 (A) Equivalent circuit of a membrane patch plus a series resistance. Instead of the transmembrane voltage (V) the voltage across the circuit (V^*) is fed back to the control amplifier. (B) Voltage changes across a membrane patch (V) a series resistance (V_s) and both components (V^*), in response to a depolarizing voltage command pulse of 50 mV. $R_s = 7$ Ω-cm^2. (C) Family of voltage records obtained from a membrane patch with a series resistance of 7 Ω-cm^2. The transmembrane voltage (continuous line) is illustrated and compared with the command potential (dotted line). To emphasize the effect of the series resistance, this computation was performed increasing the sodium and potassium conductances by a factor of 2 and the holding potential 20 mV hyperpolarized.

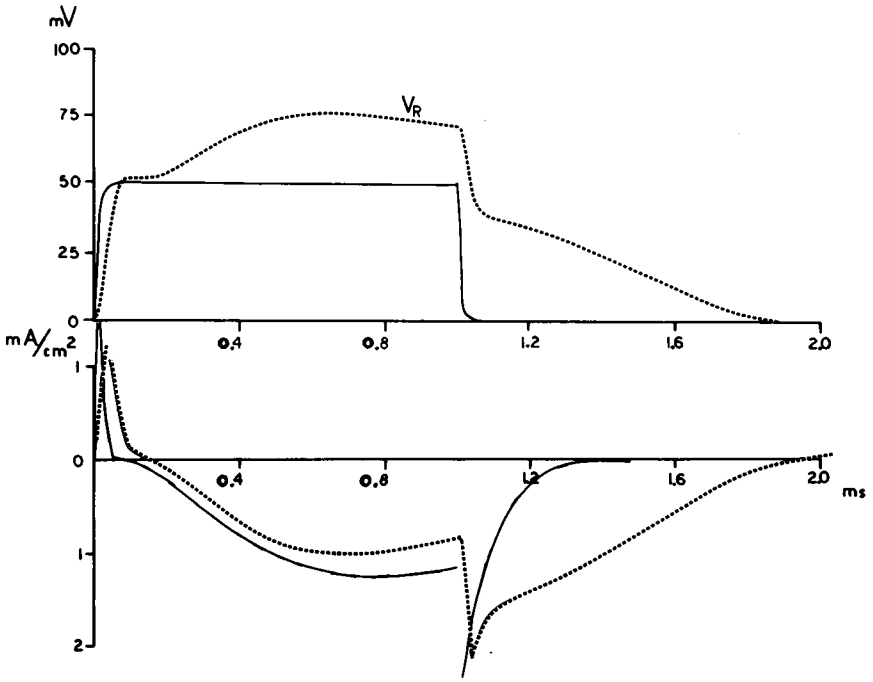

FIGURE 3 Membrane voltage and current density simulations (in response to a brief depolarization) for a membrane patch in series with a 25 Ω-cm^2 resistance (dashed line) and a 0 Ω-cm^2 resistance (solid line).

as to cause the maximum inward current to occur at a command pulse of only a few millivolts.

Another very noticeable effect of the deviation of the membrane potential from the command potential, is seen in the current "tails" resulting from repolarization to the resting level following a brief period of depolarization. For such a case, the H-H model itself gives an exponential decay of the conductance to its original value and is shown as the dashed curve in Fig. 3. The time constant of the decay is independent of the value of the sodium conductance and only depends on the repolarizing voltage. The effect of the series resistance during the repolarization can be seen in Fig. 3. Instead of returning immediately to the resting potential, the membrane remains depolarized for a prolonged period of time. The result of this depolarization is a sustained inward current that, in the current records, gives the appearance of an almost voltage-independent mechanism.

Unidimensional Cable. Because of the finite spatial extent of the cells, the membrane is not isopotential as in the membrane patch but an active cable, as previously discussed, must be used to simulate the preparation. For these simulations we used a single unidimensional cable, although it is possible that a better representation of the preparation would be a circuit where several cables, with different R_s to ground, are present. Since for these simulations the cable was divided in 20 equal segments,

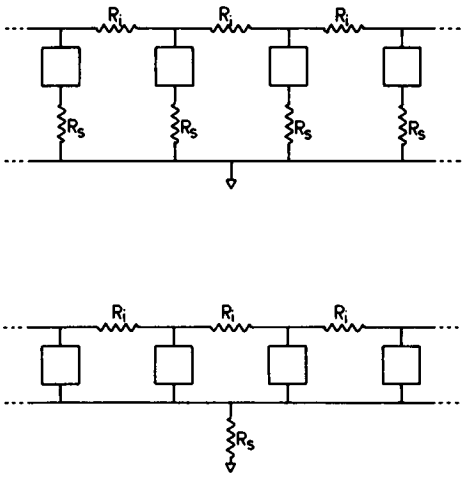

FIGURE 4 Two possible equivalent circuits for a preparation in the "node" region of a double sucrose gap. Above, each membrane patch has an associated series resistance while below is shown the series resistance lumped into a single resistor common to all patches.

we will denote the segment where current is injected, as segment I and that one where voltage is recorded, as segment R. Also, for each of these segments there are two voltage records, the transmembrane voltage V_I or V_R and the voltage across the membrane plus the series resistance V_I^* or V_R^*.

One may represent the location of the series resistance with respect to the membrane elements by more than one circuit configuration, depending on some knowledge of the tissue geometry. In axons where the series resistance is thought due to the Schwann cell layer closely wrapped around the axon membrane R_s is represented in series with each membrane element as in the upper part of Fig. 4. In a multicellular preparation, the series resistance may represent the so-called cleft resistance described by Johnson and Sommer (1967) and may be lumped as in the lower part of Fig. 4. Since in a nerve comprised of bundles of fibers both cases apply, all simulations described in this paper were performed with the circuit illustrated in the upper part of Fig. 4 that has a resistance in series with each one of the membrane segments. However for large values of series resistance (e.g. ≤ 25 Ω-cm^2) both circuit configurations give very similar results.[2]

During the voltage clamp of a unidimensional cable that has an appreciable R_s, there are two types of effects on the voltage profile along the cable. Those effects will be described first separately and then in conjunction.

(*a*) *The effect of the cable length.* The effect due to the cable length was described previously and can be summarized as follows: when a cable with a length/diameter ratio greater than 2 and $R_s = \phi$ is voltage clamped, there is an appreciable voltage

[2]For an example of lumped series resistance, applied to a cardiac muscle preparation, see Kootsey and Johnson (1972).

gradient along the cable (greater than 20% of the command pulse). This voltage gradient results because the cable segment where current is being injected deviates, in the hyperpolarizing direction during the transient phase of inward current, due to the current withdrawn by the control amplifier.

(*b*) *The effect of R_s on a single membrane patch.* If a membrane patch with series resistance is voltage clamped, the voltage across the equivalent circuit follows the command pulse; however, the voltage across the membrane itself deviates from it. The deviation, for voltage pulses below the sodium equilibrium potential, goes in the depolarizing direction during the transient phase of inward current.

When a cable with series resistance is voltage clamped, these two effects mix. During the inward current phase, the control amplifier tends to drive the voltage across segment I in the hyperpolarizing direction, while the effect of R_s is to depolarize it and since these two effects are opposite, they tend to cancel out. In other words, for each cable segment there is a value of R_s at which the effect of the longitudinal gradient and series resistance cancel each other, producing a voltage across the membrane that matches the command potential. This result is illustrated in Fig. 5, where part A shows the voltage profile for segment I with $R_s = \phi$ and part B with $R_s = 7\ \Omega\text{-cm}^2$. As can be seen in the figure, the voltage (V_I) across the membrane of segment I is now at

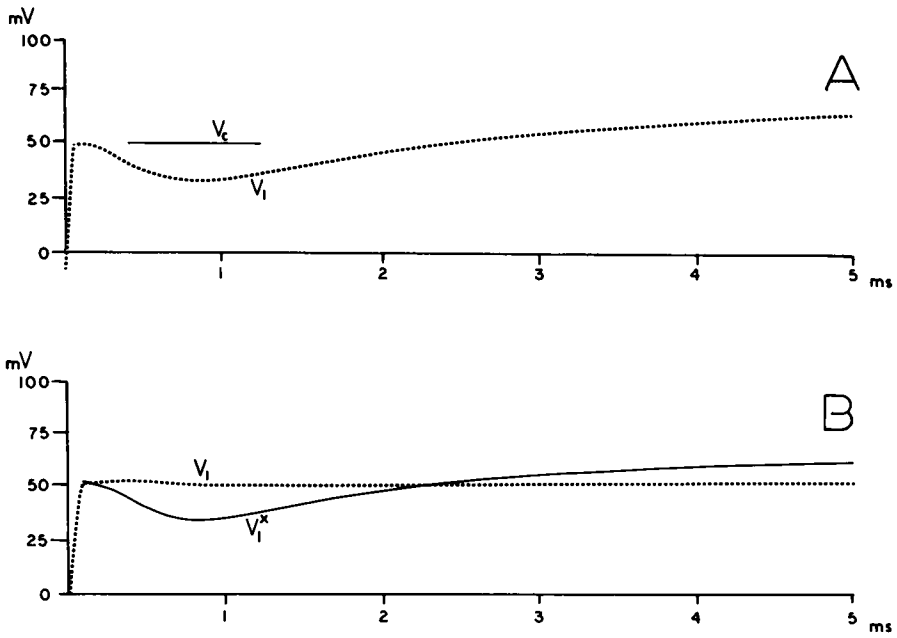

FIGURE 5 Voltage records from segment of a cable, 100 μm in diameter and 500 μm in length, plus a series resistance of 7 Ω-cm^2 associated to each one of the 20 segments. Part A shows the hyperpolarizing effect of the longitudinal gradient. In part B, the effect of the series resistance is a depolarization that moves the transmembrane voltage at segment I (V_I) up to the command potential level. The voltage across segment I plus the series resistance (V_I*) is still hyperpolarized as compared with the command potential of 50 mV (V_c).

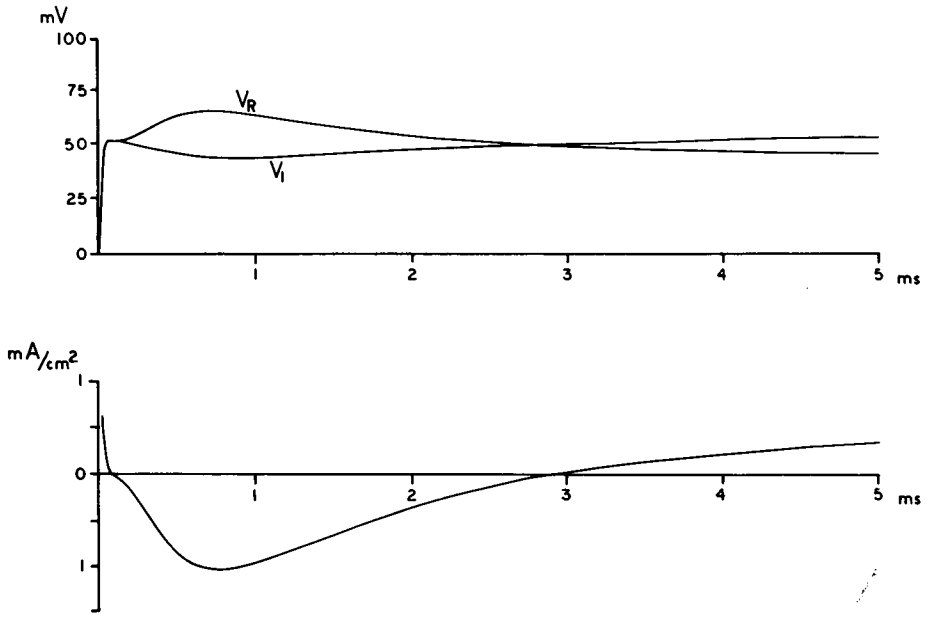

FIGURE 6 Transmembrane voltage records of the two end-segments (*I* and *R*) of a cable of 200 μm in diameter and 500 μm in length. The two transmembrane voltages are relatively close to the command potential of 50 mV. Note that the current record resulting from those potentials does not show "notches."

the command potential (V_c), while that across the membrane plus the $R_s(V_I^*)$ still deviates in the hyperpolarizing direction.

Fig. 6 shows the voltage profile of the two end-segments of a cable with series resistance. The voltage across the membrane at both ends of the cable is closer to the command potential level, since the effect of the series resistance is to change the potential at segment *I* more than at segment *R*. It was shown in the second paper of this series (Moore et al., 1975 *b*) that the reduced depolarization of segments between the current injection and the recording points, produced "notches" in the total recorded current during the period of transient inward current. The effect of the series resistance here is to offset the reduced depolarization of the membrane potential of these segments and therefore the simulated recorded current (Fig. 6 B) does not show a "notch" and it follows a more or less normal pattern.

Simulations show that, if R_s is large, the membrane may have an action potential which is free to propagate along the axon because the controlled potential is the sum of that across the membrane plus the series resistance. For reference, Fig. 7 A illustrates the system for $R_s = \phi$, showing the membrane voltage in the current input (V_I) and voltage recording (V_R) segments along with the current density which would be measured. As the series resistance is increased to 14 Ω-cm² (Fig. 7 B), the voltage deviation across the membrane begins to resemble an action potential. At an R_s of 50 Ω-cm² (Fig. 7 C), the membrane voltage approaches the unclamped form of the action poten-

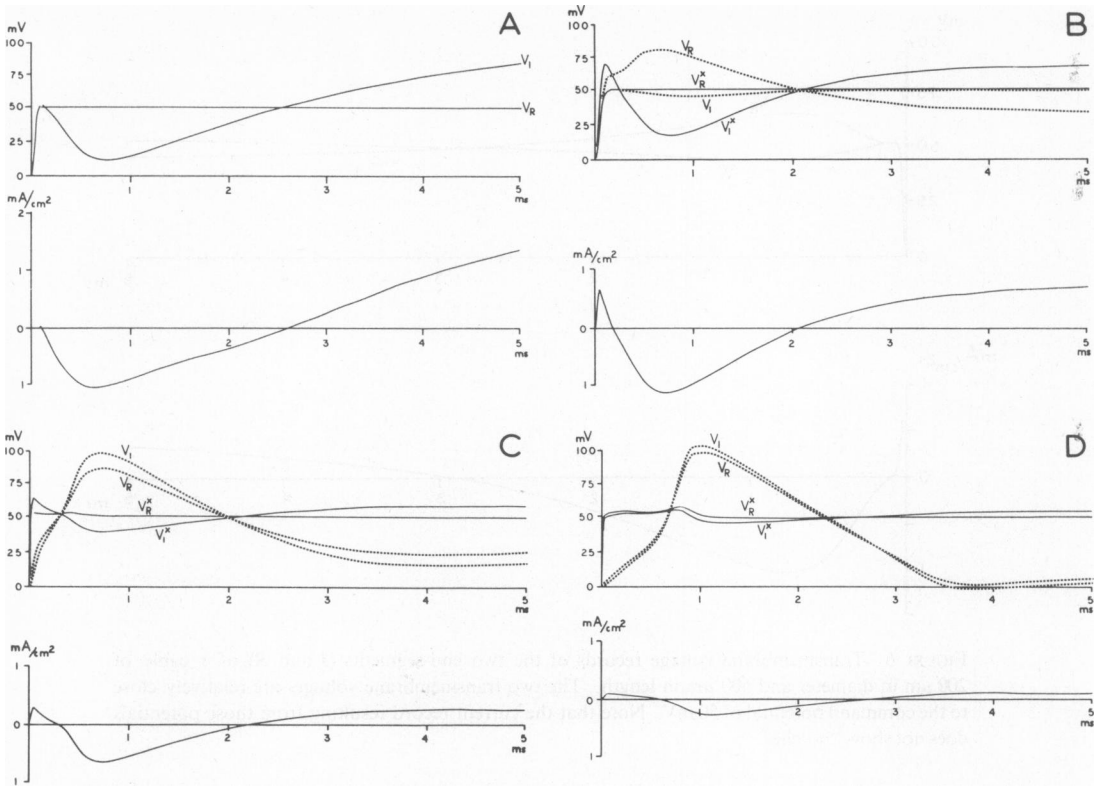

FIGURE 7 Voltage and current records for a cable 40 μm in diameter and 500 μm in length. Parts A, B, C, and D were computed with series resistances of ϕ, 14, 50, and 200 Ω-cm^2, respectively. The effect of increasing the series resistance to 14 Ω-cm^2 is to allow the transmembrane voltage of segment R to become more depolarized than the command pulse (7 B). Further increases of R_s allow all segments to generate action potentials (7 C and D). Note that none of the current records show "notches."

tial, even though its amplitude is only $\approx$ 100 mV (instead of the normal amplitude of 106 mV for the standard temperature of 6.3° C used in this computation).

For a very large series resistance (e.g. $\leq$100 Ω-cm^2), the effective source resistance is so large that action potentials in the membrane are barely discernable across the potential recording terminals.

Even under the extreme conditions of a series resistance greater than 100 Ω-cm^2, the voltage across the circuit recorded by the electrometer is a step with a small perturbation during the maximum rate of rise of the action potential. The recorded current, although much smaller in amplitude, has some resemblance to that of a voltage clamped membrane (Fig. 7 D). Kootsey and Johnson (1972) observed similar results when they simulated a single sucrose-gap voltage clamp of cardiac muscle with a large series resistance.

Another very noticeable effect of a large series resistance is that the recorded

voltage reaches the command potential level very rapidly and small values are required for the circuit capacitors to damp circuit oscillations. The circuit gives the impression of being very stable because of the absence of oscillations in the voltage records.

Shunt Pathway

We have shown that the extracellular space of a strip of smooth muscle is about 40% of the volume of the strip.[1] With this rather large extracellular space, it would be expected that a considerable amount of the current injected in a sucrose gap would flow within this space and be recorded as if it were membrane current. This argument is strengthened by the experiments of New and Trautwein (1972) on cardiac muscle. Working with a single sucrose gap on a preparation that contains approximately the same amount of extracellular space as our muscle, these authors measured ratios of intracellular to extracellular resistances that range from 0.1 to 30.

In view of these considerations about the extracellular space we were interested in analyzing the possible effects of the shunt resistance (R_{sh}). For these simulations, the distributed shunt resistance was lumped into a single resistor and the system simplified by considering only that between the current pool and the artificial node. Also, since the shunt pathway is external to the equivalent circuit representing the membrane, only the effect on a membrane patch is presented. Similar results would be obtained if a cable is used to represent the preparation.

The output of the control amplifier varies with time in order to control the voltage across the membrane, and these variations produce a shunt current with the same time dependence as that of the membrane current. For a unity ratio for intracellular and extracellular resistances, a voltage command pulse of 50 mV on the membrane *patch* produces the result shown in Fig. 8 A. The figure shows that the current recorded by the current measuring amplifier (solid line) has the same time course but is nearly twice as large as that produced by the membrane, the additional current flowing through the shunt pathway.

Shunt Plus Series Resistance

The result of a family of voltage command pulses, on a membrane with a resistance in series and a shunt pathway, is shown in Fig. 8 B. The figure demonstrates how the effect of the series resistance is masked by the current flowing through the shunt pathway. For the steady-state current the *I-V* relationship is steeper than the control and the shift of the transient current, to the left on the voltage axis, is barely distinguishable. However, the reversal potential of the transient current is not altered.

Because of the presence of the shunt pathway, the control amplifier has to supply current for the membrane as well as for the shunt pathway and therefore its output voltage climbs to very high values. The amount of current flowing through the shunt pathway may be so large as to produce an overload of an amplifier with a maximum output voltage of only ± 10 V.

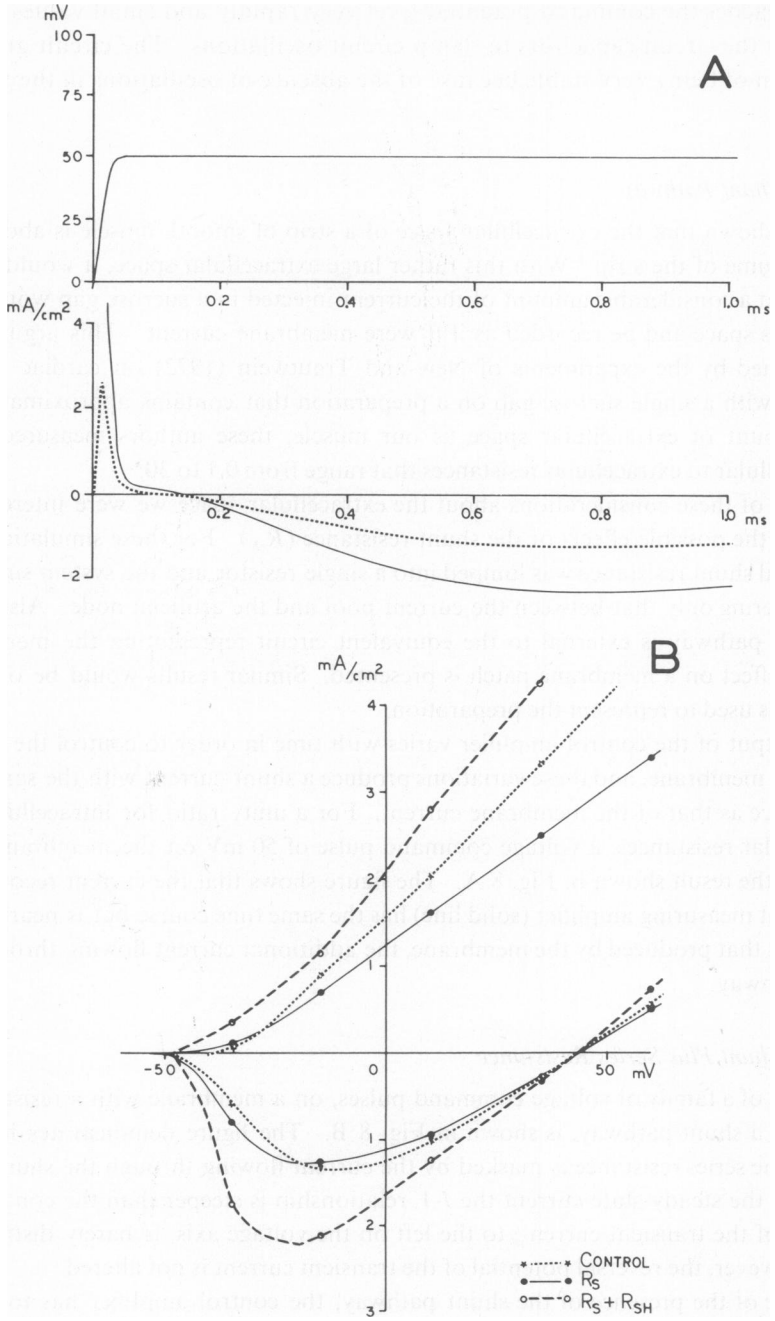

FIGURE 8 (A) Voltage and current records for a membrane plus a shunt pathway. The ratio of the internal and shunt resistances is unity. The transmembrane potential remains at the command potential level (50 mV). Due to the shunt current, the recorded current is about twice as large (continuous line) as the actual membrane current (dotted line). (B) Current-voltage relationships for a membrane patch. The dotted lines are from a membrane with no series resistance, the continuous line from a membrane plus a series resistance of 7 Ω-cm^2; and the dashed line, shows the result of the same series resistance plus a shunt resistance, for a ratio of intracellular to shunt resistance of 1. The effect of the series resistance is to shift the transient *I-V* relationship to the left along the voltage axis while the steady-state curve is shifted to the right. The presence of the shunt pathway (dashed line) masks the series resistance effects.

DISCUSSION

The values for series resistance used in the computations reported in this paper may seem extremely high when compared with the values reported for squid giant axons of 7 Ω-cm^2 (Hodgkin et al., 1952) or 3–5 Ω-cm^2 (Cole and Moore, 1960). However, in multicellular preparations, such as a bundle of small axons or a syncytium tissue (smooth or cardiac muscle), most cells are not at the surface of the strip. But even for the most superficially located cells, there are usually several layers of tissue around the strip. In a nerve trunk, individual or small bundles of fibers are surrounded by Schwann cells, and there is also a variable amount of connective tissue. In a syncytial tissue, small bundles are surrounded by connective tissue and also the strip is surrounded by connective tissue. Under these conditions, it is easy to imagine that the muscle cell membranes are separated from the recording electrodes by large resistances. Furthermore, smooth muscle cells have a large number of infoldings.[1] The cell membranes located inside these infoldings must have large series resistances associated with them.

Estimations of the series resistance in experiments ranged from values similar to even larger than those used in this paper. For example, we have measured the series resistance as 600–700 Ω-cm^2 (Ramón, 1973) in smooth muscle and in cardiac muscle similar values have been reported (600 Ω-cm^2, Beeler and Reuter, 1970; 200–600 Ω-cm^2, New and Trautwein, 1972). Since those values for series resistance are only an average, obtained in preparations containing around 1 cm^2 of surface membrane, it is quite probable that at least part of that membrane must have values of series resistance larger than those.

The simulations described in this paper indicate that, with a series resistance greater than 25 or 50 Ω-cm^2, the membrane has a propagated action potential even when the voltage recorded across the combination of membrane and series resistance is equal to the control potential. Therefore, it is to be expected that most of the preparation in the double sucrose-gap "voltage clamp" undergoes a propagated action potential.

On the other hand, it was shown (Fig. 7) that even when a portion of the preparation produces freely propagating action potentials, the recorded current resembles that of a voltage-clamped membrane in that there is a transient phase of inward current and a sustained phase of outward current. This result is easily explained by noticing that a propagated action potential contributes an insignificant fraction of the measured membrane current.

Electronic compensation for the series resistance might seem to be a good prospect. By using this compensation, values of series resistance for axons were reduced by 70% (Hodgkin et al., 1952). However, we have calculated that, in order to measure and compensate for the series resistance, the amplifiers in the feedback have to be extremely fast. We have made computations for the squid axon which indicate that the real value of the series resistance is underestimated by 1 Ω-cm^2 for every 1 μs of first order lag in the current injection and voltage measurement amplifiers.

As compared to the problems introduced by the presence of a resistance in series

with the membrane, the problems of a shunt pathway seem almost insignificant. However, it is worth noticing that since such an unknown resistance introduces an unknown current, the membrane current density cannot be known (even in the unlikely event of knowing the membrane area). These problems are present, not only in the double sucrose gap, but also in the single sucrose-gap arrangement. In conclusion, an unknown shunt pathway makes meaningless all calculations for current density or actual values of the transmembrane voltage, as recorded by the electrometer.

The "node" in the sucrose gap can be made arbitrarily narrow (measuring it at the surface of the strip) and a unidimensional cable, longitudinally placed between the current and voltage pools may not be the best representation of the preparation. Perhaps a better representation would be a "radial" cable, extending from the surface to the core of the strip. An even better representation would be a combination of longitudinal and radial cables each one having different series and shunt resistances. From the description of that possible equivalent circuit for the preparation it is clear that such a network would be even more difficult to control than the single unidimensional cable used for the simulations in this paper. We did not solve this network in our simulations, having used the single unidimensional cable as the most favorable case.

In summary, the interpretation of voltage clamp results from multicellular preparations is complicated by the presence of: (*a*) the cable effects of the preparation, (*b*) the resistances in series with the membrane, and (*c*) the shunt pathway.

An error analysis requires independent measurements of these properties together with an appropriate membrane model. It is clear that the presence of biphasic current recording and apparent voltage control does not indicate a true membrane voltage clamp.

We appreciate the contributions of Mr. E. M. Harris (in maintaining the computers operational) and Mrs. D. Munday (in typing the several drafts of these papers).

We are pleased to acknowledge the support of this work by the National Institutes of Health in the form of grants NS03437 and HD02742.

Received for publication 17 June 1974.

REFERENCES

ABE, Y., and T. TOMITA. 1968. *J. Physiol. (Lond.).* **196**:87.
ANDERSON, N. 1969. *J. Gen. Physiol.* **54**:145.
BEELER, G. W., and H. REUTER. 1970. *J. Physiol. (Lond.).* **207**:165.
COLE, K. S., and J. W. MOORE. 1960. *J. Gen. Physiol.* **44**:123.
GOLDMAN, L., and C. L. SCHAUF. 1972. *J. Gen. Physiol.* **59**:659.
HODGKIN, A. L., and A. F. HUXLEY. 1952. *J. Physiol. (Lond.).* **117**:500.
HODGKIN, A. L., A. F. HUXLEY, and B. KATZ. 1952. *J. Physiol. (Lond.).* **116**:424.
JOHNSON, E. A., and M. LIEBERMAN. 1971. *Ann. Rev. Physiol.* **33**:479.
JOHNSON, E. A., and J. R. SOMMER. 1967. *J. Cell Biol.* **33**:103.
KOOTSEY, J. M., and E. A. JOHNSON. 1972. *Biophys. J.* **12**:1496.
MOORE, J. W., F. RAMÓN, and R. W. JOYNER. 1975 *a*. *Biophys. J.* **15**:11.
MOORE, J. W., F. RAMÓN, and R. W. JOYNER. 1975 *b*. *Biophys. J.* **15**:25.

NEW, W., and W. TRAUTWEIN. 1972. *Pfluegers Arch. Eur. J. Physiol.* **334**:1.
RAMÓN, F. 1973. Ph.D. Thesis. Duke University, Durham, N.C.
ROUGIER, O., G. VASSORT, and R. STÄMPFLI. 1968. *Pfluegers Arch. Eur. J. Physiol.* **301**:91.
TARR, M., and J. TRANK. 1974. *Fed. Proc.* **33**:445.
TOMITA, T. 1966. *J. Theor. Biol.* **12**:216.